Functional Methionines in the Collagen/Gelatin Binding Domain of Plasma Fibronectin: Effects of Chemical Modification by Chloramine T†

Allen M. Miles and Robert L. Smith*

Department of Biochemistry and Molecular Biology, Louisiana State University Medical Center, Shreveport, Louisiana 71130

Received November 23, 1992; Revised Manuscript Received May 6, 1993

ABSTRACT: Chemical modification of plasma fibronectin (pFn) or its 40-kDa collagen/gelatin binding (CGB) domain by low concentrations of chloramine T (CT), a methionine-specific oxidant, caused decreased binding affinity between pFn or the isolated CGB domain and Sepharose-immobilized denatured collagen or a Texas Red-labeled CNBr fragment CB7 from the α1 chain of type I collagen. K_ds obtained by fluid-phase fluorescence polarization binding assays increased upon oxidation about 17-fold for pFn and by 4-fold for the CGB domain. Comparison of CT-oxidized and native CGB domains by endogenous tryptophan fluorescence and CD spectra gave no indication of conformational changes. ΔG_{H_2O}, the free energy of unfolding at infinite denaturant dilution, derived from guanidinium chloride denaturation curves, differed by less than 0.7 kcal/mol for the oxidized and native CGB domains, indicating essentially equivalent conformational stabilities. We show here that methionyl residues found at positions 412, 432, and 446 are the sites of the oxidative modification. Modification protection experiments carried out in the presence of gelatin demonstrated specific protection of otherwise oxidizable methionyl residues and preservation of high-affinity binding. These results implicate methionyl residues as functional in contributing to high-affinity binding interaction between fibronectin and gelatin.

Fibronectin (Fn)[1] is a large extracellular glycoprotein composed of two similar polypeptide subunits of 220–250 kDa (Hynes, 1990). The complete primary structures for human, rat, and bovine Fns which have been determined at the protein and/or cDNA level reveal greater than 90% identity (Kornblihtt et al., 1985; Skorstengaard et al., 1986). Functionally, Fn has been implicated in mediating numerous important biological activities such as cell–substratum and cell–cell adhesion, wound healing, and phagocytic clearance of colloidal debris (Akiyama & Yamada, 1987).

Fn structure is that of a modular protein containing homologous repeat sequences within a series of compact globular domains (Hynes, 1990). The collagen/gelatin binding (CGB) domain of Fn is located near the N-terminus of each subunit and may be isolated after limited proteolysis as a 38–40-kDa fragment. The domain consists of cystine-rich type I (i.e., four) and type II (i.e., two) Fn homology repeats. While type I repeats are found in other Fn globular domains, type II repeats are unique to the CGB domain and are therefore suspected of involvement in binding between Fn and collagen/gelatin (Skorstengaard et al., 1984).

Gold and Pearlstein (1979) altered several amino acid residues in Fn and tested the ability of modified Fn molecules to mediate cellular adhesion to tissue culture dishes coated with calf skin collagen. Chemical alteration of amino acids, including methionine, failed to disrupt the ability of Fn to mediate cellular adhesion. Vuento et al. (1982) showed that chemical modification of lysyl and arginyl residues significantly decreased gelatin-binding affinity in whole Fn. Modification of lysine resulted in major conformational changes (Vuento et al., 1983), whereas no conformational changes were associated with arginine-modified Fn.

In an attempt to more precisely map the site of gelatin binding in Fn, Owens and Baralle (1986) expressed amino-terminal fragments of pFn containing portions of the CGB domain as fusion proteins in *Escherichia coli*. These authors proposed that the binding site was localized within a fragment containing the type II_2 and type I_7 homology repeats. They further suggested that an intervening stretch of 14 amino acid residues (i.e., AAHEEICTTNEGVM) was critical to specific binding.

Isaacs et al. (1989) demonstrated that citraconylation of Lys residues in a 42-kDa CGB domain also abolished gelatin binding, which was restored upon removal of citraconyl groups. Since no other structural changes were detected, they concluded that specific binding to gelatin involved protonated Lys residues.

The binding of Fn to collagen is probably important in the formation of the extracellular matrix (ECM) of animals (Kleinman & Wilkes, 1982). Currently, there is great interest in the effects of both endogenous and exogenous oxidants upon the integrity of extracellular and circulating proteins (Weiss, 1989; Halliwell & Gutteridge, 1989). The nonenzymatic oxidation of methionine residues in proteins to methionine sulfoxide has been shown to occur both *in vitro* and *in vivo* and is often accompanied by loss of biological activity (Brot & Weissbach, 1983). In proteins, methionine residues may be classified into three general categories: exposed, partially exposed, and buried. Depending upon location, these exhibit differences in their susceptibility to oxidation (Beck-Speier et al., 1988; Lilova et al., 1987).

The CGB domain of Fn is slightly enriched in Met residues (Mosher, 1989), which constitute almost 3% of the residues in this region. The domain contains nine methionyl residues located at positions 289, 300, 412, 432, 446, 459, 462, 463,

† This work was supported by a grant from the U.S. National Heart, Lung and Blood Institute (HL36965). A.M. was supported by a NIH/NIGMS MARC Faculty Fellowship.

* Address correspondence to this author.

[1] Abbreviations: Fn, fibronectin; pFn, plasma fibronectin; CGB, collagen/gelatin binding; TR-CB7, Texas Red-labeled major fibronectin-binding CNBr fragment of type I collagen; CT, chloramine T; GdmCl, guanidinium chloride; PTH, phenylthiohydantoin; ECM, extracellular matrix; CNBr, cyanogen bromide; DABS-Cl, (dimethylamino)benzenesulfonyl chloride; BCA, bicinchoninic acid; PVDF, poly(vinylidene difluoride); TFA, trifluroacetic acid.

0006-2960/93/0432-8168$04.00/0

and 509. Structural domains rich in methionine have been reported in other proteins (Bernstein et al., 1989; O'Neil & Degrado, 1990). The amino acid content of signal recognition particle (SRP54) and calmodulin includes approximately 6% methionines which are located in exposed pools near the protein surface and are thought to play a key role in recognizing diverse nonpolar surfaces in other proteins (High & Dobberstein, 1991; O'Neil & Degrado, 1990). This function may be related to the flexibility of the methionyl side chain and to the polarizability of the thioether sulfur atom (Gellman, 1991). Logically, methionine residues in the CGB domain of Fn may play a similar functional role in providing a site for hydophobic interaction which may contribute to high-affinity binding to gelatin.

Initial experiments performed in our laboratory in which pFn or its proteolytically isolated CGB domain was exposed to a methionyl-specific oxidant (i.e., CT) revealed decreased binding affinity for gelatin and TR-CB7 (a Texas-Red labeled CNBr fragment CB7 of type I collagen containing a major Fn binding site). We show here that, in the absence of major conformational changes upon oxidation, methionine is implicated as contributing functionally to binding between Fn and collagen/gelatin.

We also describe the results of experiments designed to elucidate the sequence locations of CT-modified methionyl residudes, the oxidation of which directly correlates with a decrease in binding affinity for gelatin and TR-CB7. Comparison of the CNBr cleavage patterns for native and CT-oxidized CGB domains through application of SDS–PAGE, reversed-phase HPLC, and simultaneous Edman sequencing analyses has permitted the identification of three pFn methionyl residues, one or more of which we believe to be directly involved in contributing to high-affinity binding between pFn and denatured collagen.

MATERIALS AND METHODS

Chemicals. All chemicals were either of reagent grade or of the highest purity available. Urea, *N*-acetylmethionine, Trizma (Tris[hydroxymethyl]aminomethane), chloramine T (*N*-chloro-*p*-toluenesulfonamide sodium salt), formic acid (99%), dithiothreitol, 2-mercaptoethanol, glycine, and porcine skin type I gelatin were all purchased from Sigma. CNBr, BCA protein assay reagents, and Sequanal-grade 6 N HCl were from Pierce. CNBr-activated Sepharose 4B was from Pharmacia, and subtilisin was obtained from Boehringer. High-purity guanidinium chloride (GdmCl) was supplied by HEICO. 4-Vinylpyridine and *N*-ethylmorpholine were from Aldrich Chemical Co. Citrated human plasma was supplied by the Plasmapheresis Laboratory of LSU Medical Center.

Isolation and Purification of Proteins. Plasma Fn (pFn) was isolated from fresh-frozen citrated human plasma as described in detail elsewhere (Smith & Griffin, 1985). Protein concentration was determined from 280-nm absorbance using an extinction coefficient of 1.28 cm^2 mg^{-1} (Mosesson et al., 1975). Plasma Fn isolated according to this procedure yielded a product better than 90% homogeneous as determined by silver-stained SDS–PAGE on 7.5% gels. Samples were stored frozen at −70 °C.

The CGB fragment of pFn was prepared as previously described (Griffin et al., 1986). Protein concentration was determined from 280-nm absorbance employing an extinction coefficient of 1.73 cm^2 mg^{-1} determined by the methods of Edelhoch (1967). The enhanced BCA (Pierce) method was also used to verify concentrations.

Preparation of TR-CB7. Preparation of the Texas Red-labeled (Molecular Probes, Eugene, OR) cyanogen bromide fragment CB7 of type I collagen (TR-CB7) has also been previously described (Smith et al., 1988).

CNBr Cleavage of the CGB Domain. CNBr cleavage was performed as previously described with some modifications (Gross, 1967). Solutions containing about 0.5 mg of CGB domain were dialyzed versus water at 4 °C and dried. The dried sample was dissolved in 0.25 mL of deaerated 0.1 N HCl before addition of 60 μL of an acetonitrile solution containing 10 mg/mL CNBr. The final concentration of CNBr was in 50-fold molar excess over methionine. After 24 h at room temperature, the mixture was diluted 10-fold with H_2O, dried under vacuum, reconstituted in 0.5 mL of H_2O, redried, and finally diluted to 0.25 mL with H_2O. Aliquots of these CNBr digests were then analyzed by SDS–PAGE or HPLC or stored frozen at −25 °C for later analysis or chemical treatment.

Chloramine T Oxidation. Oxidation of pFn or CGB domain was performed in 50–100 mM Tris-HCl solutions, pH 8.3, at 25 °C with a molar ratio of CT to methionine at 2:1, unless stated otherwise. At the end of each oxidation, a 10-fold excess (relative to CT) of *N*-acetylmethionine was added as quencher. Controls were prepared by mixing nonoxidized CGB domain with solutions containing preincubated CT and *N*-acetylmethionine at concentrations equal to those of test samples.

SDS–Polyacrylamide Gel Electrophoresis. SDS–PAGE was carried out according to Laemmli (1970) in gels of final acrylamide concentration ranging from 7.5% to 20%.

(Dimethylamino)azobenzensulfonyl Chloride Amino Acid Analysis. Analysis of proteins and peptides for their amino acid composition was performed according to the DABS-Cl amino acid analysis procedure (Beckman Instruments).

Analysis of Protein for Methionine Sulfoxide. The procedure followed for indirect determination of methionine sulfoxide was that described by Neumann (1967). Following carboxymethylation with iodoacetic acid at pH 2.0 in 8 M urea, samples were dialyzed versus deionized water, lyophilized to dryness, and then reconstituted in 0.25–0.5 mL of 0.1 N HCl. Aliquots were then prepared for amino acid analysis.

Fluorescence Measurements. Both fluorescence emission spectra and fluorescence polarization binding assays were performed on a SLM Instruments Model SPF-500C spectrofluorometer using software supplied by the manufacturer. Fluorescence emission spectra for 1.3×10^{-6} M solutions of CGB domains dissolved in 50 mM Tris-HCl, pH 7.4, were normally recorded in 1-cm path length quartz cuvettes at 25 °C. Excitation wavelength was 280 nm with 20-nm band pass, and emission was recorded between 300 and 500 nm with a band pass of 5 nm.

The SLM SPF-500C was also equipped with a polarization accessory used in binding assays and incorporates the L-format for measurements of polarization. The fluorescence polarization binding assays employing TR-CB7 were performed with excitation at 580 nm and emission at 620 nm as described by Smith et al. (1988).

Circular Dichroism Spectra. Circular dichroism (CD) spectra of the CGB domain in 10 mM phosphate buffer, pH 7.1, were recorded at 25 °C on an Aviv Model 62DS circular dichroism spectrometer. Sample concentrations ranged between 3.0 and 6.0 μM with 0.1-cm path length. Ellipticity was measured over the wavelength range from 184 to 280 nm with a resolution of 0.5 nm.

GdmCl Denaturation Curves. The intrinsic fluorescence of the CGB domain increased upon unfolding. Denaturation curves were constructed from fluorescence intensity data expressed as a ratio of emission recorded at 360 nm to that at 320 or 350 nm with excitation at 280 nm (Ingham & Brew, 1992). Aliquots of freshly prepared 6 M GdmCl in 50 mM Tris-HCl, pH 7.4, were diluted with the appropriate volume of 50 mM Tris-HCl, pH 7.4, to provide GdmCl at a specific molar concentration. To each vial an equal aliquot of a stock protein solution was added, yielding a final protein concentration of 1.3×10^{-6} M in 1-mL aliquots. Solutions were then incubated in a constant-temperature bath at 25 °C for 1 h prior to making fluorescence measurements.

Reduction and Alkylation of CNBr-Cleaved CGB Domains. CNBr-cleaved CGB domains were alkylated by carboxymethylation employing iodoacetic acid or pyridylethylated with 4-vinylpyridine (Hirs, 1967; Tarr, 1986).

Simultaneous Edman Degradation of CNBr-Cleaved CGB Domains. After treatment of native and CT-oxidized CGB domains with CNBr, samples were vacuum-dried and stored at −25 °C under argon until sequencing. Edman analyses were performed by the Core Laboratories of Louisiana State University Medical Center in New Orleans. Simultaneous Edman analysis of peptide mixtures provided a means by which identification and semiquantitation of CNBr cleavage at specific methionines in the CGB domain could be accomplished. The feasibility of this approach was ascertained using mixtures of commercially purchased peptides. N-Terminal residues and concentrations of the mixture were selected to correspond to those expected for complete CNBr cleavage at all nine methionyl residues in the nonoxidized CGB domain. Except for CNBr cleavage, these samples were carried through the identical steps used to prepare actual samples. Data obtained for Edman degradation analysis of these mixtures yielded first-cycle recoveries of N-terminal residues of between 60% and 90% of expected amounts.

Electroblots of SDS–PAGE Gels. These were prepared according to the procedure described by Matsudaira (1987).

HPLC Isolation and Purification of Peptides. Separation of CNBr-derived peptides was performed on a Vydac 2.4- × 25-mm C-18 reversed-phase analytical column with a linear gradient of 1%/min with 95% acetonitrile–5% H_2O (0.1% TFA) and H_2O (0.1% TFA) at a 1 mL/min flow rate.

Protection of Methionines against CT Oxidation. Samples of pFn or native CGB domain were applied to separate 1-mL gelatin–Sepharose affinity columns and then exposed to solutions of CT. Columns employed for testing the protection of methionines in whole pFn and CGB domain were preconditioned with several column volumes of $(3–6.5) \times 10^{-4}$ M CT in 50 mM Tris-HCl, pH 8.3. The presence of excess oxidant in the eluent was confirmed by qualitative colorimetric detection with 1.0 M KI. For each test, separate control columns were prepared. These were exposed to CT only during the pretreatment step and not after binding pFn or the CGB domain. All columns were thoroughly washed with several volumes of 50 mM Tris-HCl solutions of pH 7.4 and 8.3 before loading of protein samples and after exposure to CT. Final elution of bound protein was accomplished with 4 M urea in 50 mM Tris-HCl, pH 7.4. Samples were collected as 0.5-mL fractions and monitored for protein content by absorbance at 280 nm. Pooled fractions were then dialyzed overnight versus 50 mM Tris-HCl, pH 7.4. Estimated recoveries of protein ranged between 60% and 90%.

The elution flow rate for all columns was approximately 0.33 mL/min. Gelatin-bound proteins (i.e., pFn or CGB domain) were exposed to 2 mL of a CT solution which meant total exposure times of about 6 min. In the case of pFn, 0.5 mL of a 6.5×10^{-6} M solution (i.e., 1.63 mg of Fn) was added to the control and test columns, whereas 0.5 mL of a 20.4×10^{-6} M solution (i.e., 0.41 mg) of the CGB domain was used. Following 20 h of dialysis versus 50 mM Tris-HCl, pH 7.4, control and CT-exposed samples were assayed for TR-CB7 binding.

ANALYSIS OF DATA

Fluorescence Polarization Measurements. Binding constants were estimated from titration data employing a nonlinear least-squares computer fit to

$$\Delta P = (\Delta P_{max}/2\mathrm{TR})[\mathrm{TR} + nF + K_d - [(\mathrm{TR} + nF + K_d)^2 - 4nF(\mathrm{TR})]^{1/2}] \quad (1)$$

where ΔP is the change in fluorescence polarization, TR represents the concentration of TR-CB7, F is pFn or CGB domain concentration, n is the number of binding sites, assumed to be 2 for pFn and 1 for CGB domain, and K_d is the apparent dissociation constant. The validity of the expression rests on a number of basic assumptions which have been explained elsewhere (Ingham et al., 1990). The computer program used for nonlinear regression analysis of titration data was Enzfitter (Leatherbarrow, 1987). K_ds obtained after a large number of determinations performed in 20 mM Tris-HCl/130 mM NaCl, pH 7.4, at 25 °C occurred at 6.2 ± 0.1 nM (n = 56) and 25.0 ± 0.2 nM (n = 100) for native pFn and CGB domain, respectively.

Calculation of Free Energy of Unfolding. The equilibrium constant (K_u) for the two-state model of protein denaturation in which only the native and the unfolded states are populated may be calculated as

$$K_u = (F_n - F)/(F - F_u) \quad (2)$$

where F is the observed fluorescence ratio and F_n and F_u are the fluorescence ratios of the native and denatured forms of the protein (Pace, 1986). Thus the free energy of unfolding can be calculated as

$$\Delta G_u = -RT \ln K_u = -RT \ln (F_n - F)/(F - F_u) \quad (3)$$

where ΔG_u is the free energy of unfolding at a GdmCl concentration, R is the universal gas constant, 1.987 cal mol^{-1} K^{-1}, and T is the temperature in kelvins. Estimation of the free energy of unfolding in the absence of denaturant, ΔG_{H_2O}, was determined from a linear extrapolation of data from the transition region of denaturation curves fitted to

$$\Delta G_u = \Delta G_{H_2O} - m[\mathrm{GdmCl}] \quad (4)$$

where m is the slope and is a measure of the dependence of ΔG_u on denaturant concentration. Equation 5 is derived by combining eqs 3 and 4 (Jackson & Fersht, 1991):

$$F = F_n - (F_n - F_u)\frac{\exp(m[\mathrm{GdmCl}] - \Delta G_{H_2O})/RT}{1 + \exp(m[\mathrm{GdmCl}] - \Delta G_{H_2O})/RT} \quad (5)$$

Estimation of ΔG_{H_2O} for protein samples was calculated from unfolding data by nonlinear regression analysis using the Enzfitter computer program and eq 5, which does not contain parameters to correct for changes in fluorescence ratio observed before and after the unfolding midpoint transition, $D_{50\%}$.

RESULTS AND DISCUSSION

Figure 1 shows elution profiles of native and CT-treated CGB domains from gelatin–Sepharose. Almost 60% of the

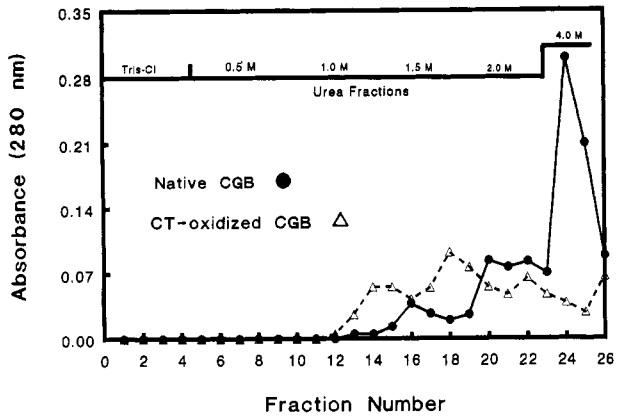

FIGURE 1: Comparison of the gelatin–Sepharose elution profiles of subtilisin-generated native and CT-oxidized CGB domains. One-milliliter gelatin–Sepharose affinity columns were loaded with 0.5 mL of a 20.4×10^{-6} M solution of the CGB domain dissolved in 50 mM Tris-HCl, pH 7.4. Bound protein was eluted with urea in 50 mM Tris-HCl, pH 7.4. The oxidized sample had been exposed to 3.4×10^{-4} M CT in 50 mM Tris-HCl, pH 8.3, at 25 °C for 3 min before being quenched with 0.1 N *N*-acetylmethionine. The concentration of CT used represented a 2:1 molar ratio of CT to methionine.

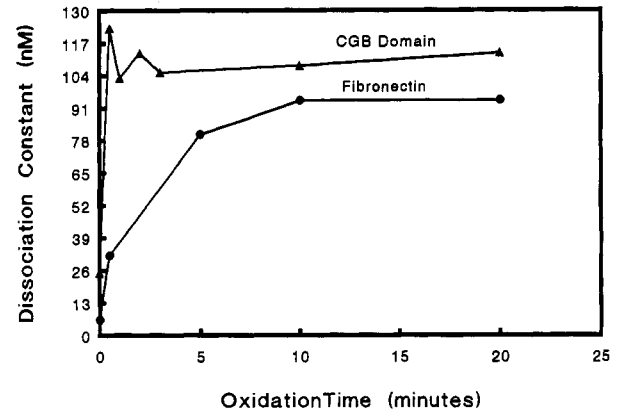

FIGURE 2: Increase in dissociation constant as a function of CT oxidation time for pFn and CGB domain. A 0.25-mL aliquot of a 6.5×10^{-6} M solution of pFn or a 0.5-mL aliquot of 20×10^{-6} M solution of the CGB domain was allowed to react with CT at a 2:1 molar ratio (CT to methionine) in 50 mM Tris-HCl, pH 8.3, at 25 °C for the indicated time periods. At the end of each period, a 10-fold excess of *N*-acetylmethionine was added as quencher. Samples were then diluted with 20 mM Tris-HCl/130 mM NaCl, pH 7.4, to a final concentration of 8.0×10^{-7} M and 14.0×10^{-6} M for pFn and the CGB domain, respectively. Dissociation constants were obtained employing these solutions in separate fluorescence polarization binding assays with TR-CB7.

total recovered CT-treated CGB domain eluted from affinity columns in solutions containing less than 2 M urea, whereas only 30% of the native protein was removed in urea solutions at concentrations below 4 M. Under equivalent experimental conditions, the binding of pFn to a similar gelatin–Sepharose column also decreased significantly following CT oxidation (data not shown).

Time Course Oxidation. Chemical modification of either protein with CT resulted in higher K_ds for TR-CB7 binding, which suggests a functional role for methionine in the binding interaction between pFn and TR-CB7.

Using CT-oxidized samples of pFn or CGB domain as titrant, data for dissociation constants are shown plotted versus oxidation time in Figure 2. The effects of oxidation on binding occurred rapidly at reaction time of less than 5 min. The apparent K_d obtained for binding of CT-oxidized pFn to TR-CB7 increased 17-fold higher than that of untreated Fn. The

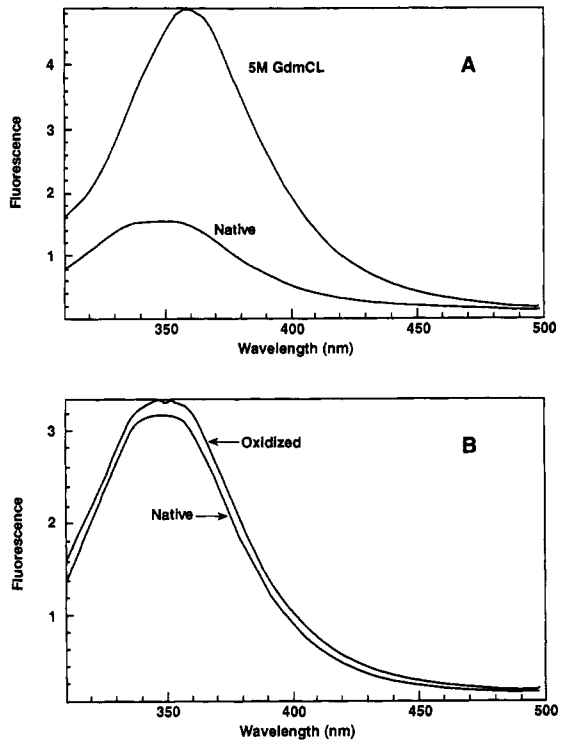

FIGURE 3: Comparison of fluorescence emission spectra for native and GdmCl-denatured nonoxidized CGB domains (panel A) and nonoxidized and CT-oxidized CGB domains (panel B). **Panel A**: Emission spectra were recorded as described in Materials and Methods. The excitation wavelength was set at 280 nm and emission was scanned from 300 to 500 nm. Solutions contained 1.3×10^{-6} M native CGB domain in either 50 mM Tris-HCl, pH 7.4, or 50 mM Tris-HCl, pH 7.4, plus 5 M GdmCl. The sample containing 5 M GdmCl was allowed to stand at 25 °C for 1 h before the emission spectrum was recorded. **Panel B**: Comparison of emission spectra for native and 3-min CT-oxidized CGB domains. Protein concentration was 2.0×10^{-6} M in 50 mM Tris-HCl, pH 7.4.

apparent binding constant determined for the oxidized CGB domain increased sharply to a value approximately 4-fold higher than that of the untreated CGB domain. In both cases apparent K_ds approached a value close to 100 nM without complete loss of binding. We believe this suggests equivalent binding affinities for oxidized pFn and CGB domain resulting from the loss of a common high-affinity binding component.

Because oxidation similarly affected the binding of both intact pFn molecule and the CGB domain to immobilized gelatin or TR-CB7, the CGB domain was selected as an appropriate model to further investigate the effects of oxidation by CT on pFn binding to gelatin.

Fluorescence Emission and Circular Dichroism Spectra Data. The CGB domain contains 8 Trp and 21 Tyr residues. If decreased binding upon oxidation of methionyl residues is a direct result of major alterations in protein conformation, these should be detectable as perturbations in the intrinsic Trp fluorescence. As expected (Isaacs et al., 1989), unfolding of the CGB domain in concentrated solutions of GdmCl increased emission intensity by 3–4-fold, accompanied by a red shift in the emission wavelength maximum from between 340 and 350 nm to approximately 360 nm. Panel A of Figure 3 shows emission spectra recorded for solutions of the CGB domain in the absence and presence of 5 M GdmCl. Quantum yield for 280-nm excitation of native CGB domain in the absence of GdmCl was estimated at 0.005. Although this value increased about 6-fold to 0.033 for spectra recorded in the presence of 5 M GdmCl, spectral yields are far below that expected for complete unfolding of the CGB domain. Isaacs

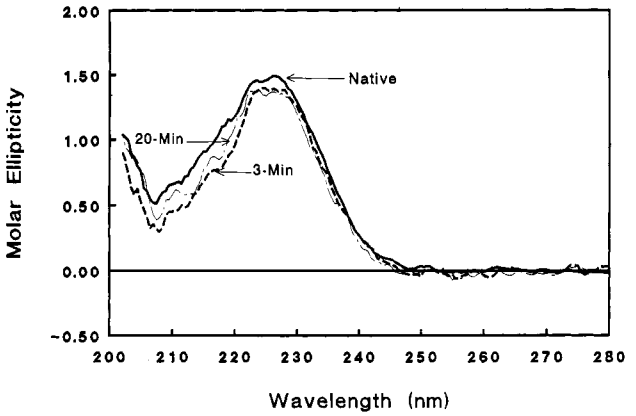

FIGURE 4: Circular dichroism spectra of native and CT-oxidized CGB domains. Spectra represent averages of three replicate scans from 280 to 203 nm at 0.5-nm resolution in 0.1-cm path length cells. Protein samples were in 10 mM phosphate buffer, pH 7.1. The concentration of the native sample was 6.0×10^{-6} M, whereas that for the oxidized samples was 2.8×10^{-6} M. Oxidized samples were treated with CT at a 2:1 (CT to methionine) ratio for 3 or 20 min. Dissociation constants obtained from fluorescence polarization binding assays were 50 nM and 100 nM for the 3- and 20-min oxidized samples, respectively. The maximum positive molar ellipticity at 225 nm was essentially equivalent, yielding values of $1.5 \times 10^{+5}$ deg M^{-1} cm^{-1} for the native sample and $1.3 \times 10^{+5}$ deg M^{-1} cm^{-1} for oxidized CGB domains.

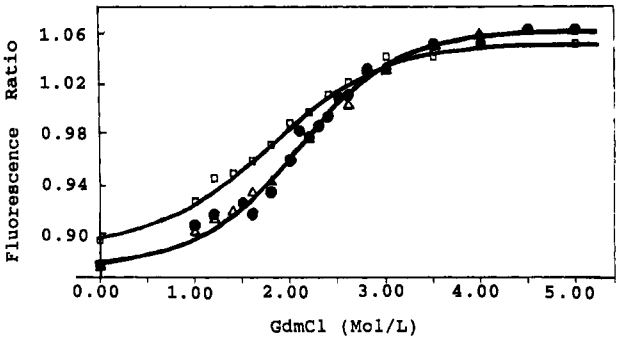

FIGURE 5: Conformational stability of CGB domains following specific chemical modification by CT. GdmCl denaturation curves were constructed for native (●) and oxidized (30 min, △; 60 min, □) CGB domains from measurements made at 25 °C of change in the 360/350 nm fluorescence ratio with excitation at 280 nm. Solutions contained 1.3×10^{-6} M CGB domain in 50 mM Tris-HCl, pH 7.4, plus the corresponding concentration of GdmCl. Each point represents a mean value obtained from five denaturation curve analyses. Coincidence of data for the native sample with data for oxidized samples suggests nearly equivalent free energies of unfolding. The solid lines drawn through data points represent the Enzfitter computer program best fit of experimental data. The curves drawn through data for the native and 30-min oxidized samples were indistinguishable. Dissociation constants for TR-CB7 binding of the native and 30-min oxidized CGB domains were calculated to be 28 nM and 120 nM, respectively. The K_d for the 60-min oxidized CGB domain was undeterminable. Values calculated for ΔG_{H_2O}, $D_{50\%}$, and m are reported in Table I.

et al. (1989) reported an 8-fold increase in the maximum emission intensity in conjunction with complete unfolding of a similar thermolysin-generated 42-kDa CGB domain from pFn. We infer from this that, under the experimental conditions used to generate the upper curve in panel A of Figure 3, partial unfolding of the CGB domain is achieved.

In panel B of Figure 3, comparison is made of fluorescence emission spectra recorded for native and CT-oxidized CGB domains. Emission maxima for both spectra occurred between 340 and 350 nm with emission intensities within 6% of each other. The spectra are nearly indistinguishable, indicating no major changes in the hydrophobicity of the environment surrounding Trp residues and thus no major conformational changes in the CGB domain upon CT oxidation. Therefore, it follows that the increase in K_d noted for TR-CB7 binding is directly related to changes in the polarity of methionyl side chains upon conversion to sulfoxide.

Figure 4 shows plots of circular dichroism data obtained for native and CT-oxidized CGB domains. Ellipticity varied in a concentration-dependent manner, yet CD spectra produced maximum molar ellipticities measured at 225 nm of about $1.5 \times 10^{+5}$ and $1.3 \times 10^{+5}$ deg M^{-1} cm^{-1} for native and oxidized domains, respectively. These are essentially equivalent values and corroborate evidence from fluorescence emission data that no major conformational changes occur upon CT oxidation.

Thus, in the absence of evidence for significant conformational changes, these data implicate methionyl residues as functionally contributing to high-affinity binding between pFn and collagen/gelatin.

GdmCl Denaturation Curves and Conformational Stability. Figure 5 displays results of changes in fluorescence emission ratios as a function of GdmCl concentration. The fluorescence intensity ratio for the native protein underwent distinct monophasic increase between 2 and 3 M GdmCl, diagnostic of a one-step unfolding transition. This allowed calculation and comparison of the free energies of unfolding, ΔG_{H_2O} (Pace, 1975, 1986), for native and oxidized fragments. This transition probably corresponds to unfolding of the more labile homology repeats and apparently involves only two conformational states: the native and some stable intermediate, probably one in which the two type II and type I_8 repeats are unfolded (Litvinovich, 1991).

Table I: Derived Denaturation Data for Native and Oxidized CGB Domains

sample	oxidation time[a] (min)	ΔG_{H_2O}[b] (kcal/mol)	m (kcal mol^{-1} M^{-1})	$D_{50\%}$ (mol/L)	$\Delta(\Delta G_{H_2O})$[c] (kcal/mol)
1[d]	0.0	2.44 ± 0.16	0.99 ± 0.06	2.45	0.00
2	30.0	2.23 ± 0.09	0.96 ± 0.04	2.33	+0.12
3	60.0	1.85 ± 0.09	1.04 ± 0.04	1.78	+0.68

[a] Time of exposure to chloramine T. [b] Values shown represent the mean ± standard error. Standard errors indicate the accuracy of estimated free energy values. [c] $\Delta(\Delta G_{H_2O}) = 0.5\,(m_{native} + m_{oxidized})\Delta D_{50\%}$. [d] Native protein.

A ΔG_{H_2O} value of 2.44 kcal/mol agrees well with a reported value of 2.33 kcal/mol determined for a similar chymotryptic-derived 42-kDa CGB domain (Isaacs et al., 1989). Corrections made to account for increases in the fluorescence ratio before and after the unfolding transition resulted in less than a 20% increase in ΔG_{H_2O} for the native protein.

Recently (Ingham & Brew, 1992), a ΔG_{H_2O} value of approximately 5 kcal/mol was determined under reducing conditions at a higher temperature for GdmCl denaturation of a similar thermolysin-generated 42-kDa CGB domain. This value is comparable to the values of 5–15 kcal/mol obtained for complete unfolding of globular proteins. It is probable that the lower 2.44 kcal/mol which we observed represents partial unfolding of the CGB domain under milder conditions.

Table I contains mean free energy of unfolding values calculated for the native and oxidized samples. Comparison of these reveals an insignificant decrease in the free energy of unfolding of 0.12 kcal/mol upon mild CT oxidation. The largest change noted here for heavily oxidized CGB samples is less than 0.7 kcal/mol. The reaction conditions for this sample were 60-min oxidation time and a 20:1 molar ratio of

CT to methionine. Coincidence of denaturation data in Figure 5 for native protein with that for a 30-min oxidized sample suggests little, if any, structural destabilization upon oxidation. Only in the case of the more vigorously oxidized sample was there minor noncoincidence of denaturation curve data.

Extent of Methionine Oxidation by CT. In order to ascertain the extent of oxidation (i.e., the number of methionines converted to sulfoxide), comparisons were made between amino acid analysis data obtained for native and oxidized CGB domains before and after CNBr cleavage. In addition to homoserine, hydrolysates of the CNBr-cleaved native protein still contained methionine, indicating up to two noncleaved methionyl peptide bonds per native molecule. This failure of CNBr cleavage in the native protein could result from prior spontaneous oxidation of methionine to sulfoxide during sample preparation, since methionine sulfoxide is converted back to methionine during acid hydrolysis (Shechter, 1975). Alternatively, methionyl residues which are inaccessible to CNBr could account for incomplete cleavage. In support of the latter, Litvinovich et al. (1991) demonstrated extraordinary conformational stability of portions of the CGB domain (e.g., type I_6).

Total elimination of methionine from hydrolysates of CNBr-cleaved native protein was accomplished only when cleavage was performed in the presence of 140 mM 2-mercaptoethanol. This raises the question that, in addition to reducing disulfide bonds, 2-mercaptoethanol might also reduce preexisting methionine sulfoxide and thus allow CNBr cleavage. To resolve this question, an alternative procedure was used which involved specific differential chemical modification of methionyl residues by treatment with iodoacetic and performic acids (Neumann, 1967). Amino acid analyses of native CGB domains treated according to this procedure gave no indication of preexisting methionine oxidation. On the basis of these tests, it appeared that the presence of residual methionine after treatment was due to failure of cleavage at extraordinarily stable and/or inaccessible sites within the structure of the native protein. Later, the sequence locations of the two noncleaved sites were identified as Met289 and Met300 by other biochemical methods.

The amount of residual methionine observed in the analysis of oxidized protein was increased by approximately 3 mol of methionine/mol of protein. Failure to cleave was thus the result of conversion of methionines to sulfoxides by CT. The accompanying increase in K_d for TR-CB7 binding indicates that one or more methionyl residues are involved in binding between Fn and gelatin.

The data obtained at this point do not permit differentiation between the selective stoichiometric oxidation of these specific methionyl residues and the nonspecific, partial oxidation at more than three sites.

HPLC Analysis of CNBr-Cleaved Native and Oxidized CGB Domains. We anticipated that modification of specific methionyl residues in the CGB domain by chemical oxidation would alter the CNBr cleavage pattern which could be detected by other biochemical methods (e.g., HPLC peptide maps).

The CGB domain isolated as a 40-kDa subtilisin proteolytic fragment consists of 315 amino acid residues beginning at Val262 and ending at Ser576 (numbers refer to residue positions in an intact polypeptide chain of human pFn) (Mosher, 1989). The nine peptides anticipated from complete CNBr cleavage of the native domain are listed in Table II, along with their amino-terminal sequences.

A typical HPLC peptide map of the CNBr-cleaved, reduced, and alkylated native CGB domain is shown in Figure 6 (panel A). Five or six cycles of Edman sequencing were performed on each of the peaks. The N-terminal sequences found matched those of six of the expected CNBr fragments (Table II, last column). Multiple peaks having the same N-termini

Table II: CNBr Peptides of the CGB Domain[a]

peptide	residues	length (amino acids)	N-terminal sequence	HPLC peak no.[b]
1	Val262–Met289	28	VYQPQP...	VI
2	Gln290–Met300	11	QWLKTQ...	
3	Leu301–Met412	112	LCTCLG...	
4	Lys413–Met432	20	KWCGTT...	VII, VIII
5	Ala433–Met446	14	AAHEEI...	I, II
6	Tyr447–Met459	13	YRIGDQ...	III, IV
7	Gly460–Met462(463)	3	GHM	
8	Arg464–Met509	46	RCTCVG...	X
9	Leu510–Ser576	67	LNCTCF	IX, XI, XII

[a] Listed are the nine peptides anticipated for complete CNBr cleavage of the native CGB domain. Also listed are the expected N-terminal sequences. [b] N-Terminal sequences found for each peak from Figure 6 matched the expected sequences as shown. Sequence data for peak V was ambiguous and probably comprised a mixture of other fragments.

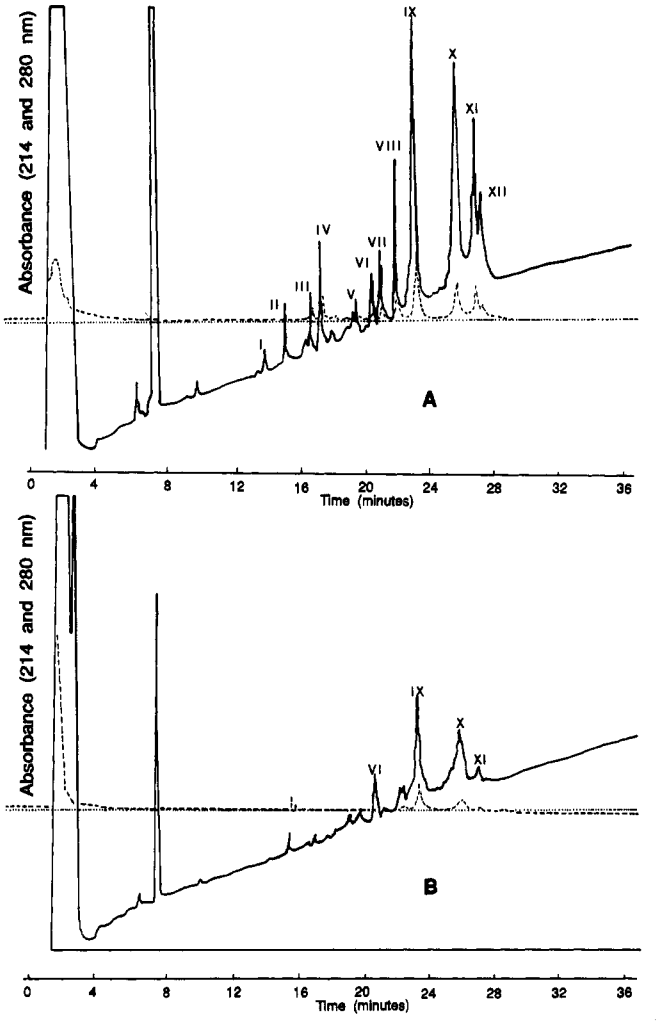

FIGURE 6: HPLC chromatograms of native (panel A) and CT-oxidized (panel B) CNBr-cleaved CGB domains. Samples were chromatographed on a Vydac C18 reversed-phase analytical column. The mobile-phase gradient of 95% acetonitrile–H_2O (0.1% TFA) and H_2O (0.1% TFA) was automatically controlled at a flow rate of 1 mL/min. The oxidized sample was treated with CT for 20 min at a 2:1 molar ratio (i.e., CT to methionine). TR-CB7 binding assay analysis performed with this sample yielded a K_d of about 160 nM. Detection of chromatographic peaks was accomplished by absorbance measurements at 214 (—) and 280 nm (- - -). Roman numerals are labels to identify peaks and are also listed in the last column of Table II beside the expected peptide with the same N-terminal sequence.

represent incomplete cleavage products of the expected peptides. Also, there are three N-linked glycosylation sites in the CGB domain, at positions 399, 497, and 511. Differences in glycosylation also may have caused variable retention times for the three glycopeptides but this aspect was not investigated further.

The tripeptide GHM, produced by cleavage at residues 459 and 463, was not recovered in HPLC peptide maps. Peptides generated by cleavage at positions 289, 300, and 412 should have resulted in fragments of 11 and 112 residues in length. However, none of the individually sequenced major chromatographic peaks had N-termini corresponding to cleavage at 289 and 300, suggesting that peak VI represents the N-terminal 151-residue fragment from Val262 to Met412.

Chemical oxidation of methionine residues in the native CGB domain altered the CNBr cleavage pattern and hence the elution profile of HPLC chromatograms. Figure 6 (panel B) is a HPLC peptide map for a 20-min-oxidized, CNBr-cleaved, reduced, and alkylated CGB domain. As anticipated, fewer peaks were evident, apparently the result of cleavage failure at sites now containing methionine sulfoxide residues. The absence of major peaks previously detected in peptide maps for the native domain (Figure 6, panel A) suggests specific chemical modification of the adjacent methionines. Again, the roman numerals located above each peak are also listed in Table II and identify the N-termini determined for the remaining peaks. The amount of the N-terminal peptide (i.e., VYQPQP...) and peptides generated by CNBr cleavage at positions 462/463 and 509 appeared relatively unaffected by the oxidative chemical treatment. In contrast, the amount of peptide in peaks corresponding to cleavage at positions 412, 432, and 446 were significantly reduced.

To determine the ability of HPLC-isolated peptide to compete for TR-CB7 binding, K_ds were obtained from separate binding assays performed in the presence of 5–10-fold molar excesses of the individual peptides. At least two of these peptides (peaks I and II) had an N-terminal sequence beginning with AAHEEI.... This sequence, between Met432 and Met446, was identified by Owens and Baralle (1986) as critical to gelatin binding. However, the effects of these purified peptides on binding of CGB to TR-CB7 were not significant, indicating that competition did not occur. This further supports the importance of intact methionyl residues to high-affinity binding in that no contiguous sequence of amino acids absent of Met was able to compete with native noncleaved CGB domain.

SDS–PAGE Analysis of CNBr-Cleaved Native and CT-Oxidized CGB Domains. Figure 7 (panel A) shows a reduced SDS–PAGE analysis of intact CGB, along with CNBr-cleaved native and CT-oxidized CGB domains. SDS–polyacrylamide gels of the native CNBr-cleaved domain (lane 3) yielded four major bands corresponding to molecular masses between 10 and 22 kDa, whereas the CT-oxidized CNBr-cleaved domain (lane 4) exhibited six major bands with molecular masses between 10 and 27 kDa. As shown in Figure 2, the effects on TR-CB7 binding of CT oxidation of the CGB domain occurred rapidly, suggesting that critical methionyl residues are readily accessible to the reagent. SDS–polyacrylamide gels of CNBr-cleaved samples of CGB domain which had been oxidized for time periods of 30 s–50 min were indistinguishable. However, for the longer oxidation times (i.e., >50 min) other, slower migrating bands appeared, evidently the result of more extensive oxidation (data not shown).

On the basis of electrophoretic mobility, the four faster migrating bands (i.e., bands labeled 1–4) in lanes 3 and 4 of

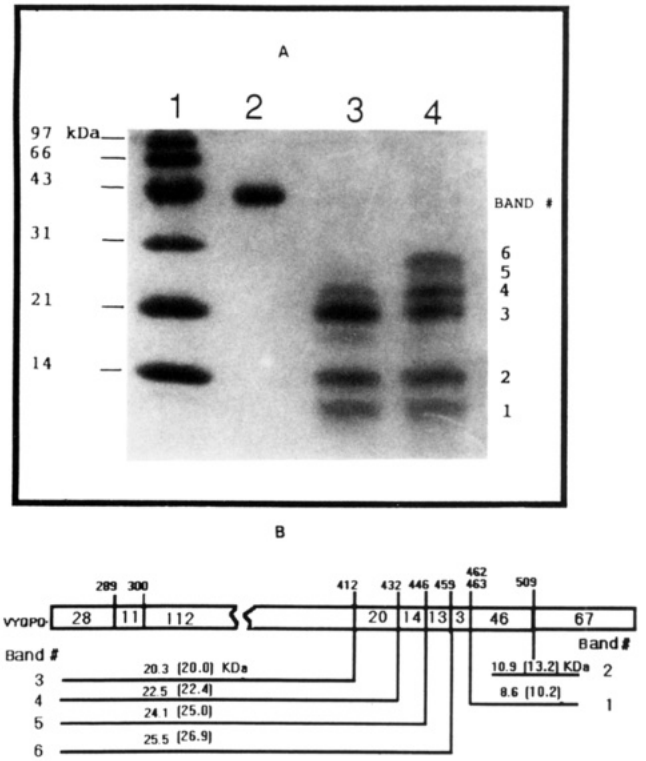

FIGURE 7: SDS–PAGE analysis of native and CT-oxidized CNBr-cleaved CGB domains (**panel A**) and schematic diagram of the relative locations of methionines in the CGB domain (**panel B**). **Panel A**: Oxidation was performed for 20 min as described in Materials and Methods. Lane 1 contains molecular mass markers. Lane 2 shows native noncleaved CGB domain. Lane 3 illustrates the typical band migration pattern on 15% gels for native CNBr-cleaved CGB domain. CT-oxidized CNBr-cleaved CGB domain is shown in lane 4. Numbers adjacent to bands are identification labels referred to in the text and are also listed in panel B. Bands were visualized with Coomassie Blue stain. **Panel B**: The rectangular shape represents the CGB domain. Numbers printed above the rectangle are sequence locations of the nine methionyl residues as they occur in the intact pFn molecule. Numbers inside the rectangles represent the residue length of CNBr-derived peptides. Numbers on the lines next to band numbers correspond to calculated and apparent (in parentheses) molecular masses of the corresponding peptide.

Figure 7 (panel A) appeared to represent equivalent peptides. On the other hand, bands 5 and 6 in lane 4 were not present in gels of the CNBr-cleaved native CGB domain (lane 3). These results were expected, since specific chemical modification of the native domain with CT should prevent CNBr cleavage at oxidized methionyl residues, generating larger, slower-migrating peptides.

Panel B of Figure 7 depicts the relative positions of the nine methionyl residues found in the native domain and the sizes of anticipated peptides generated by complete CNBr cleavage. Sequence data for HPLC-isolated peptides previously suggested failure of CNBr to cleave at positions 289 and 300. However, cleavage at six (i.e., 412, 432, 446, 462/463, and 509) of the remaining seven positions was confirmed by this method. The tripeptide located between positions 459 and 463 was not detected and was probably lost during sample workup.

CNBr digestion of the native CGB domain should result in the generation of peptides containing 20, 14, 13, 3, 46, and 67 amino acid residues. Failure of CNBr cleavage at sites 289 and 300 should produce a peptide of 151 residues. The smaller peptides of less than 46 residues were not detected by SDS–PAGE, however, probably due to their sizes and/or difficult staining. Attempts to visualize these by SDS–PAGE on 20% gels by silver staining were unsuccessful.

Table III: Simultaneous Edman Analysis of Native CNBr-Cleaved CGB Domain

peptide	size (amino acids)	Met position	residue relative yield[a] cycle 1	cycle 2	cycle 3	cycle 4	cycle 5	cycle 6
1	28	NT	V, 1.0	Y, 1.0	Q, 1.0	P, 1.0	Q, 1.0	P, 1.0
2	11	289	Q, 0.0	W[b]	L, 0.1	K, 0.0	T	Q
3	112	300	L	C, nd[c]	T	C, nd	L, 0.0	G
4	20	412	K, 0.8	W	C, nd	G	T	T, 0.5
5	14	432	A, 1.6	A, 1.8	H, 0.5	E, 0.6	E, 0.7	I, 0.7
6	13	446	Y, 0.7	R, 0.7	I, 0.7	G	D, 0.5	Q
7	3	459	G, 0.9	H, +++[d]	M, 0.0			
8	46	462/463	R, 0.4	C, nd	T	C, nd	V, 0.8	G
9	67	509	L	N[e], nd	C, nd	T, 0.7	C, nd	F, 0.9

[a] Mean values for $n = 4$ analyses. [b] Relative yield data not reported for residues which are not unique. [c] Not detected; cystines remain oxidized. [d] Detected but not quantitated. [e] Suspected glycosylation site.

Table IV: Simultaneous Edman Analysis of CT-Oxidized CNBr-Cleaved CGB Domain

peptide	size (amino acids)	Met position	residue, relative yield[a] cycle 1	cycle 2	cycle 3	cycle 4	cycle 5	cycle 6
1	28	NT	V, 1.0	Y, 1.0	Q, 1.0	P, 1.0	Q, 1.0	P, 1.0
2	11	289	Q, 0.2	W	L, 0.1	K, 0.1	T	Q
3	112	300	L	C, nd	T	C, nd	L, 0.1	G
4	20	412	K, 0.2	W	C, nd	G	T	T, 0.3
5	14	432	A, 0.7	A, 0.6	H, 0.2	E, 0.5	E, 0.6	I, 0.7
6	13	446	Y, 0.2	R, 0.2	I, 0.2	G	D, 0.3	Q
7	3	459	G, 0.8	H, 0.03	M, 0.1			
8	46	462/463	R, 0.07	C, nd	T	C, nd	V, 0.6	G
9	67	509	L	N, nd	C, nd	T, 0.9	C, nd	F, 0.7

[a] Mean values for $n = 2$ analyses.

The larger peptides of 46, 67, and 151 residues were easily confirmed as shown in Figure 7 (panel A). Tentative identification of these was accomplished on the basis of molecular mass comparisons. The calculated masses (based on actual sequences) of the three peptides ranged between 9 and 20 kDa, including the addition of a mass of 3500 Da for glycosylation sites (Ingham et al., 1989). The apparent masses (i.e., numbers enclosed by parentheses in Figure 7, panel B) of bands 1, 2, and 3 corresponded closely to calculated masses for the 46-, 67-, and 151-residue peptides, respectively.

Cleavage failure at positions 412 and 446 in the oxidized CGB domain should minimally increase the mass of the 151-residue peptide by 2200 Da and lead to the appearance of a band with a molecular mass of about 22 kDa (band 4). Concomitantly, a decrease in the amount of peptide present in band 3 should occur. Band 4 then apparently represents a peptide of 171 amino acid residues and therefore signaled failure of cleavage at methionyl 412 after oxidation. It follows, therefore, that bands 5 and 6 result from further extension of the 171-residue peptide due to failure of CNBr to cleave at other positions.

N-Terminal sequences of peptides in individual bands from PVDF membrane electroblots from SDS–polyacrylamide gels of CNBr-cleaved native and oxidized CGB domains were determined by Edman analyses. Bands 1 and 2 yielded the N-terminal sequences RCTCVG and LNCTCF, which correspond to cleavage at positions 462/463 and 509, respectively. Bands 3–6 all had the N-terminal sequence VYQPQP..., confirming the prediction of their identity as cleavage-failure extensions of the peptide represented by band 3.

Simultaneous Edman Analysis of Native and Oxidized CGB Domains. Isolation of CNBr fragments by SDS–PAGE or HPLC followed by partial sequencing failed to account for all of the expected cleavage products. We therefore utilized the approach of subjecting CNBr digestion mixtures of CGB domains to gas-phase Edman sequencing through six cycles to determine the presence of amino acid derivatives unique to the N-terminus of expected fragments in each cycle. Yields for each cycle were normalized to the corresponding residue in the N-terminal peptide, VYQPQP....

Table III shows mean values of normalized derivative yields obtained from four separate simultaneous Edman analyses of native CNBr-cleaved CGB domain. In the first Edman cycle, the presence of the N-terminal peptide is represented by Val, whereas failure of CNBr cleavage at methionyl residues 289 and 300 is indicated by the absence of Gln and Lys in cycles 1 and 4 for peptide 2 and the absence of Leu in cycle 5 for peptide 3, respectively. The failure of CNBr to cleave at both Met289 and Met300 was considered evidence that these methionyls may be inaccessible to reagent due to extraordinary conformational stability. As mentioned, amino acid analyses of CNBr-cleaved native CGB domain showed two residual methionines per CGB domain. These residues are located in the type I_6 homology repeat which is extremely conformationally stable (Litvinovich, 1991), probably limiting access of CNBr to these residues.

The high levels of PTH-Ala in the first Edman cycle were mostly likely due to more efficient PTH derivatization and recovery of PTH-Ala relative to PTH-Val.

In Table III, sequence-unique N-terminal residues for four of the remaining seven CNBr peptides (i.e., peptides 4–7) appear at expected levels in the first cycle and thus substantiate cleavage at corresponding adjacent methionines (i.e., Met412, Met432, Met446, and Met459). Although the level of PTH-Arg in the first cycle from peptide 8 is lower than values noted for other residues, the appearance of a sequence-unique PTH-Val in good yield in the fifth cycle confirms CNBr cleavage at position 462/463. Cleavage at position 509 is indicated by the appearance of sequence-unique residues for peptide 9, PTH-Thr and PTH-Phe in cycles 4 and 6.

Table IV presents similar data for CT-oxidized CGB domain. Fluorescence polarization TR-CB7 binding assay analysis yielded an apparent K_d of 160 nM. Again, failure of CNBr cleavage at Met289 and Met300 is indicated by the

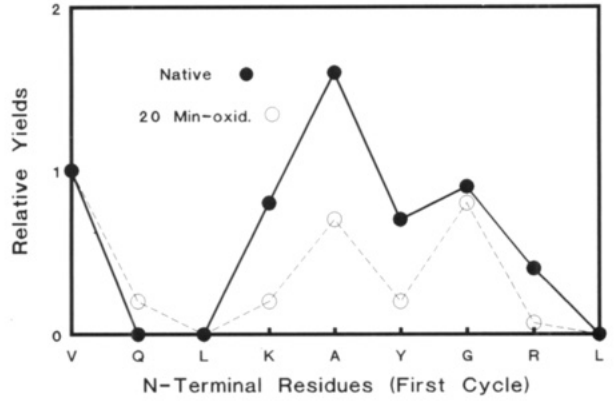

FIGURE 8: Plot of N-terminal residues (first cycle) versus relative yields. Data were taken from Tables III and IV.

absence of sequence-unique residues which correspond to peptides 2 and 3, respectively. The relative yields of N-terminal sequence-unique residues for peptides 4, 5, and 6, which correspond to cleavage at positions 412, 432, and 446, respectively, decreased by 60–80%. The relative yield of sequence-unique PTH-Gly in the first cycle for peptide 7 again indicates cleavage at Met459. Again, CNBr cleavage at position 462/463 to generate peptide 8 is demonstrated by the presence of sequence unique PTH-Val in cycle 5. Also, peptide 9, generated by cleavage at Met509, is confirmed by PTH-Thr in cycle 4 and PTH-Phe in cycle 6.

A comparison of data in Tables III and IV reveals changes in CNBr cleavage as indicated by large decreases in the relative amounts of N-terminal derivative yields following chemical modification of the CGB domain by CT. Figure 8 plots the relative yields versus N-terminal residues (first cycle) taken from Tables III and IV. The plot illustrates the magnitude of changes which result from oxidation. Moreover, the identity of methionine residues most affected by oxidative chemical modification, namely, 412, 432, and 446, become evident.

Variability observed in the first-cycle yields of PTH-Gly with individual oxidized samples (data not shown) suggests that the cleavage for which it is an indicator is variable and that Met459 may also be modified by CT.

We conclude that Met412, Met432, Met446, and perhaps Met459 of the CGB domain are sites of CT oxidation which accompany the observed decrease in gelatin and TR-CB7 binding.

Protection of Methionines from Modification. To further test the hypothesis of direct interaction of methionines in the protein–protein interaction, we wished to determine whether or not high-affinity TR-CB7 binding activity of pFn and the CGB domain is preserved upon exposure to CT after formation of the pFn–gelatin or the CGB–gelatin complex. Accordingly, samples of pFn and native CGB domain were bound to separate gelatin–Sepharose affinity columns, exposed to CT, and then eluted and tested for evidence of oxidative modification.

pFn samples yielded dissociation constants of 8.7 nM for control samples and 8.5 nM for those exposed to CT on gelatin columns. Variations were within experimental error, indicating equivalent binding affinities for TR-CB7.

Dissociation constants obtained for CGB domains treated as described were 16 nM and 22 nM for the control and CT-exposed samples, respectively. A separate duplicate experiment employing the CGB domain yielded a K_d for a control sample of 20 nM, whereas a value of 27 nM was obtained for a gelatin-protected sample. These are equivalent values within experimental error. Thus, the high-affinity binding properties

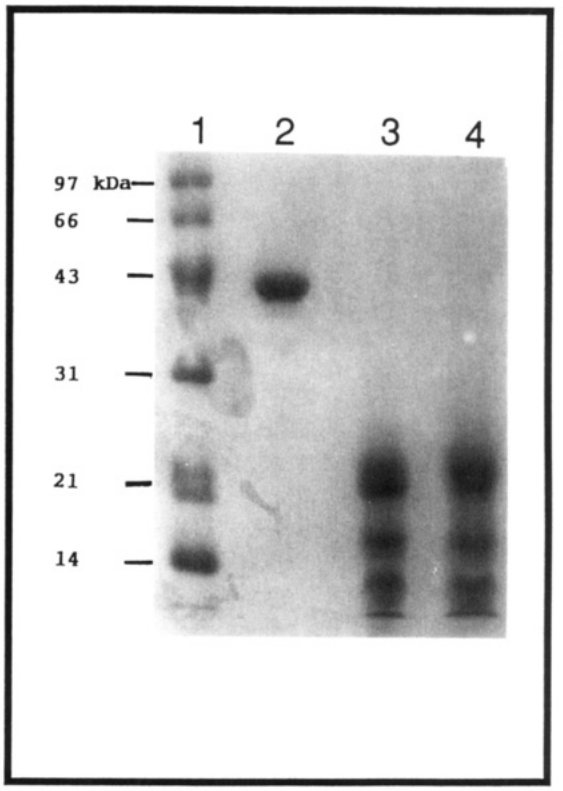

FIGURE 9: SDS–PAGE analysis of gelatin-protected CNBr-cleaved CGB domain. Samples of CGB domain were exposed to 2 mL of 3.0×10^{-4} M CT while bound to 1-mL gelatin–Sepharose affinity columns at 25 °C (flow rate 0.3 mL/min). Lane 1, molecular mass markers; lane 2, noncleaved CGB domain; lane 3, CNBr-cleaved control; lane 4, CT-exposed gelatin-protected CNBr-cleaved CGB domain.

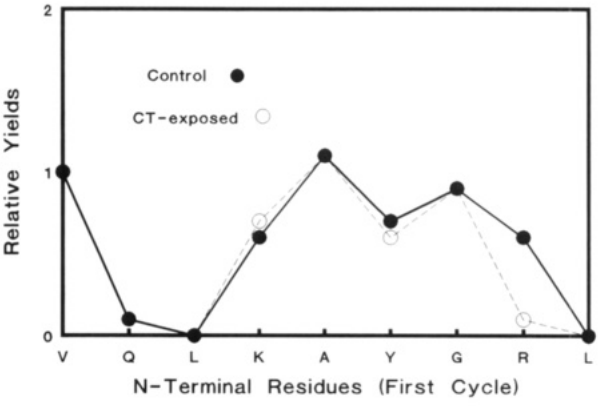

FIGURE 10: Plots of N-terminal residues (first cycle) versus relative yields for control and gelatin-protected CT-exposed CNBr-cleaved CGB domains.

of both whole pFn and CGB domains were preserved when CT oxidation was carried out in the presence of gelatin.

The CGB domains from the latter experiments above were also subjected to CNBr cleavage and SDS–PAGE analysis. The band migration patterns, shown in Figure 9, were indistinguishable, yielding four major bands as shown previously for native samples.

A comparison of simultaneous Edman analyses of the CNBr-cleaved control and CT-exposed gelatin-protected domains yielded data for first-cycle derivative yields shown plotted in Figure 10. The sequence data were indistinguishable and are similar to those previously shown in Table III for the native CGB domain. These data confirm the protection by gelatin of methionines against oxidative modification.

Failure of CT to oxidize methionyl residues in the CGB domain under normal experimental conditions while bound to immobilized gelatin demonstrated specific protection of otherwise oxidizable (exposed) methionyl residues and futher implies their location proximal to the gelatin binding site and their possible direct involvement in pFn binding to gelatin.

CONCLUSIONS

We have demonstrated that chemical modification of pFn or its isolated CGB domain by the methionine-specific reagent chloramine T causes decreased binding affinity for denatured collagen and TR-CB7. Moreover, this decreased affinity occurs in the absence of major structural change or destabilization of the isolated CGB domain. We propose that these results demonstrate a functional role for one or more Fn methionines in the binding interaction between Fn and collagen.

The CGB domain is slightly enriched in methionine, constituting almost 3% of the total amino acid composition. Other proteins having structural domains rich in methionines which serve as sites for recognition of diverse nonpolar surfaces in other proteins have been recently reported (Bernstein et al., 1990; High & Dobberstein, 1991). Methionyl residues in the CGB domain of pFn may play a similar functional role in providing sites for interaction with hydrophobic sequences in collagen and thus contribute to binding.

Conversion of the thioether sulfur of methionine to sulfoxide results in conversion from a more to a less hydrophobic side chain which may as a result become more solvent exposed. If oxidation of methionine to methionine sulfoxide increases solvent exposure of otherwise buried residues, this should be reflected in changes in ΔG_{H_2O}. The small changes in ΔG_{H_2O} noted here when comparing native and modified CGB domains would correspond to the transfer of less than one methionyl side chain per molecule of protein (Pace, 1975; Nozaki & Tanford, 1970). Instead, these small changes in free energy after oxidation more probably reflect the additive effects of very minor conformational adjustments made by already partially exposed methionyl residues.

Through application of a combination of biochemical analyses, we have identified the sequence locations of methionyl residues specifically modified by CT oxidation. Methionyl residues located at positons 412, 432, and 446 are apparently the primary sites of the oxidative modification. Methionyl 459 may also be variably modified under similar conditions. It appears that conversion of one or more of these residues to the methionyl sulfoxide is directly related to the observed effect of decreased binding affinity. These results imply that the side chains of Met412, Met432, and Met446 must be at least partially solvent-exposed near the surface of the CGB domain.

Recent investigations (Seidah et al., 1987; Esch et al., 1983) have identified two bovine seminal fluid proteins, PDC-109 and BSP-A_3, which display marked affinity for denatured collagen (Banyai et al., 1990). Each protein is mainly composed of two Fn-like type II homology repeats. In the second type II repeat of these proteins, a methionyl residue is found in a sequence position similar to that of Met412 in type II_2 of pFn. Banyai and Patthy (1991) presented evidence of the involvement of Fn-like type II repeats in a 72-kDa procollagenase in its binding to denatured collagen. This protein contains three tandemly arranged type II repeats. The third type II repeat contains a methionyl residue located one position upstream of the equivalent sequence location of Met412 in human pFn (Collier et al., 1988).

Using NMR spectroscopy, Constantine et al. (1992a) were able to identify the tertiary location of this conserved methionyl residue in the second Fn-like type II homology repeat of the PDC-109 protein. Their model showed this methionyl residue in a shallow hydrophobic depression on the PDC-109 protein surface. This depression was recognized as a potential site for binding the Leu- and Ile-containing sequence near the collagenase-sensitive site in collagen. Our data are consistent with this observation.

The solution structure of the seventh Fn type I homology repeat and of a Fn 13-kDa gelatin-binding fragment containing the type I_6 and type II_1 repeats have also been deduced from ^1H NMR studies (Baron et al., 1990; Constantine et al., 1992b). The tertiary and secondary solution structures of type I and type II homology repeats are largely conserved (Constantine et al., 1992b). Met432 is located in the connecting amino acid sequence between the type II_1 and the type I_7 repeats. Although present NMR data does not allow for unambiguous assignment of the Met432 side chain, connecting sequences are solvent-exposed and are thus susceptible to proteolytic cleavage (Ingham et al., 1989; Litvinovich et al., 1991, 1992). Baron et al. (1990) described the structure of the type I_7 repeat as consisting of antiparallel β-sheets which enclose a hydrophobic core of three highly conserved aromatic residues (i.e., Tyr447, Trp453, and Trp475). It is therefore likely that the side chain of Met446 is directed away from the hydrophobic core but toward the protein surface.

We propose that one or more of the human pFn methionines located at positions 412, 432, and 446 act cooperatively in conjunction with other hydrophobic and hydrophilic interactions to contribute to binding between Fn and collagen.

ACKNOWLEDGMENT

The authors would like to thank Mike Czyca for C-terminal determination of the CGB domain and Dr. Jeffery Nelson for CD spectra. We also thank Dr. Kenneth Ingham for his helpful suggestions and discussions during the course of this work.

REFERENCES

Akiyama, S., & Yamada, K. M. (1987) *Adv. Enzymol. Relat. Areas Mol. Biol. 59*, 1–57.
Banyai, L. & Patthy, L. (1991) *FEBS Lett. 282*, 23–25.
Banyai, L., Trexler, M., Koncz, S., Gyenes, M., Sipos, G., & Patthy, L. (1990) *Eur. J. Biochem. 193*, 801–806.
Baron, M., Norman, D., Willis, A., & Campbell, I. D. (1990) *Nature (London) 345*, 642–646.
Beck-Speier, I., Leuschel, L., Luippold, G., & Maier, K. L. (1988) *FEBS Lett. 227*, 1–4.
Bernstein, H. D., Poritz, M. A., Strub, K., Hoben, P. J., Brenner, S., & Walter, P. (1989) *Nature (London) 340*, 482–486.
Brot, N., & Weissbach, H. (1983) *Arch. Biochem. Biophys. 223*, 271–281.
Collier, I. E., Wilhelm, S. M., Eisen, A. Z., Marmer, B. L., Grant, G. A., Seltzer, J. L., Kornberger, A., He, C., Bauer, E. A., & Goldberg, G. I. (1988) *J. Biol. Chem. 263*, 6579–6587.
Constantine, K. L., Madrid, M., Banyai, L., Trexler, M., Patthy, L., & Llinas, M. (1992a) *J. Mol. Biol. 223*, 281–298.
Constantine, K. L., Brew, S. A., Ingham, K. C., & Llinas, M. (1992b) *Biochem. J. 283*, 247–254.
Edelhoch, H. (1967) *Biochemistry 6*, 1948–1954.
Gellman, S. H. (1991) *Biochemistry 30*, 6634–6636.
Gold, L. I., & Pearstein, E. (1979) *Biochim. Biophys. Acta 581*, 237–251.
Griffin, C. A., Calaycay, J., Shively, J., & Smith, R. L. (1986) *Thromb. Res. 43*, 469–477.
Gross, E. (1967) *Methods Enzymol. 11*, 238–255.

Halliwell, B., & Gutteridge, J. (1989) *Free Radicals in Biology and Medicine*, 2nd ed., Clarendon Press, Oxford, England.
High, S., & Dobberstein, B. (1991) *J. Cell Biol. 113*, 229–233.
Hynes, R. (1990) *Fibronectins*, Springer-Verlag, New York.
Ingham, K. C., & Brew, S. A. (1992) *Proteins: Struct., Funct., Genet. 12*, 180–187.
Ingham, K. C., Brew, S. A., & Migliorini, M. M. (1989) *J. Biol. Chem. 265*, 16977–16980.
Ingham, K. C., Brew, S. A., & Atha, D. H. (1990) *Biochem. J. 272*, 605–611.
Isaacs, B. S., Brew, S. A., & Ingham, K. C. (1989) *Biochemistry 28*, 842–850.
Jackson, S. E., & Fersht, A. R. (1991) *Biochemistry 30*, 10428–10435.
Kleinman, H. K., & Wilkes, C. M. (1982) in *Collagen in Health and Disease* (Weiss, J. B., & Jayson, M. I., Eds.) Churchill Livingston, New York.
Kornblihtt, A., Umezawa, K., Vibe-Pedersen, K., & Baralle, F. E. (1985) *EMBO J. 4*, 1755–1759.
Laemmli, U. (1970) *Nature (London) 227*, 680–685.
Leatherbarrow, R. J. (1987) *Enzfitter*, Elsevier Science Publishers BV, The Netherlands.
Lilova, A., Kleinschmidt, T., & Nedkov, P. (1987) *Biol. Chem. Hoppe-Seyler 368*, 513–519.
Litvinovich, S. V., Strickland, D. K., Medved, L. V., & Ingham, K. C. (1991) *J. Mol. Biol. 217*, 563–575.
Litvinovich, S. V., Novokhatny, V. V., Brew, S. A., & Ingham, K. C. (1992) *Biochim. Biophys. Acta 1119*, 57–62.
Matsudaira, P. (1987) *J. Biol. Chem. 262*, 10035–10038.
Mosesson, M. W., Chen, A. B., & Huseby, R. M. (1975) *Biochim. Biophys. Acta 386*, 509–524.
Mosher, D. (1989) *Fibronectin*, Academic Press, San Diego, CA.
Neumann, N. P. (1967) *Methods Enzymol. 11*, 487–490.
Nozaki, Y., & Tanford, C. (1970) *J. Biol. Chem. 245*, 1648–1652.
O'Neil, K. T., & Degrado, W. F. (1990) *Trends Biochem. Sci. 15*, 59–64.
Owens, R. J., & Baralle, F. E. (1986) *EMBO J. 5*, 2825–2830.
Pace, C. N. (1975) *Crit. Rev. Biochem. 3*, 1–43.
Pace, C. N. (1986) *Methods Enzymol. 131*, 266–280.
Shechter, Y., Burstein, Y., & Patchornik, A. (1975) *Biochemistry 14*, 4497–4502.
Skorstengaard, K., Thogersen, H. C., & Petersen, T. E. (1984) *Eur. J. Biochem. 140*, 235–243.
Skorstengaard, K., Jensen, M. S., Sahl, P., Petersen, T. E., & Magnusson, S. (1986) *Eur. J. Biochem. 161*, 441–453.
Smith, R. L., & Griffin, C. A. (1985) *Thromb. Res. 37*, 91–101.
Smith, R. L., Stafford, P. R., & Griffin, C. A. (1988) *J. Cell Biol. 107*, 808a.
Tarr, G. E. (1986) in *Methods of Protein Microcharacterization* (Shively, J. B., Ed.) pp 162–163, Humana Press, Totowa, NJ.
Vuento, M., Salonen, E., Osterlund, K., & Stenman, U. (1982) *Biochem. J. 201*, 1–8.
Vuento, M., Stenman, U., Salonen, E., Osterlund, K., & Kuusela, P. (1983) *Mol. Immunol. 20*, 149–153.
Weiss, S. J. (1989) *N. Engl. J. Med. 320*, 365–376.